MicroRNA-10b expression in node-negative breast cancer-correlation with metastasis and angiogenesis

XIA LIU[1,2], YONG GUAN[1], LI WANG[1] and YUN NIU[1]

[1]Tianjin Medical University Cancer Institute and Hospital, National Clinical Research Center of Cancer, Key Laboratory of Breast Cancer Prevention and Therapy, Tianjin Medical University, Ministry of Education, Tianjin 300060; [2]Department of Oncology, General Hospital of Tianjin Medical University, Tianjin 300052, P.R. China

Received March 6, 2017; Accepted August 10, 2017

DOI: 10.3892/ol.2017.6914

Abstract. Metastasis accounts for the majority of cases of mortality in patients with axillary lymph node-negative (ANN) breast cancer. Angiogenesis is an essential component of the metastatic pathway. Studies regarding microRNA (miR)-10b expression in patients with ANN breast cancer and the function of angiogenesis in breast cancer remain scarce. The present study was performed in order to determine the biological significance of miR-10b, and investigate the association between miR-10b and microvessel density (MVD) measured in ANN breast cancer. miR-10b expression and immunohistochemical analysis for MVD were assessed in 195 patients with ANN of invasive ductal carcinoma, including 65 cases with distant metastasis 'poor group', and 130 cases without any recurrence 'good group'. miR-10b expression was higher in the 'poor group' (73.8%) compared with that in the 'good group' (51.5%; P=0.003). Multivariate logistic regression demonstrated that miR-10b retained independent prognostic significance for distant metastasis along with MVD and vascular invasion. Among 195 patients, miR-10b expression was significantly associated with tumor grade, tumor size and molecular subtypes (P<0.05). In addition, miR-10b expression was positively associated with the MVD count (r=0.370; P<0.001), tumor grade (r=0.168; P=0.019) and tumor size (r=0.175; P=0.014). The results of the current study suggest that miR-10b is a useful marker for predicting metastasis and angiogenesis in ANN breast cancer.

Correspondence to: Dr Yun Niu, Tianjin Medical University Cancer Institute and Hospital, National Clinical Research Center of Cancer, Key Laboratory of Breast Cancer Prevention and Therapy, Tianjin Medical University, Ministry of Education, West Huanhu Road, Ti Yuan Bei, Hexi, Tianjin 300060, P.R. China
E-mail: yunniu20000@126.com

Abbreviations: ANN, axillary lymph node-negative; MVD, microvessel density; ISH, *in situ* hybridization; IDC, invasive ductal carcinoma; IHC, immunohistochemical; HER2, human epidermal growth factor receptor 2; AJCC, American Joint Committee on Cancer; ER, estrogen-receptor; PR, progesterone-receptor

Key words: breast cancer, microRNA-10b, metastasis, angiogenesis

Introduction

Although the prognosis of patients with axillary lymph node-negative (ANN) breast cancer was relatively good, approximately one-third of them experienced disease recurrence after treatment (1-3). Among recurrence, distant metastasis accounted for 90% of the mortality causes in these ANN patients. Angiogenesis was an essential component of the metastatic pathway, which was elicited and regulated by a number of factors, such as the extracellular microenvironment and endothelium-associated small non-coding RNAs, known as microRNAs.

MicroRNAs (miRNA/miR) are small non-coding RNAs (18-23 bp in size) generated by the consecutive activity of two RNAseIII enzymes, DROSHA and DICER (4). They regulate gene activity by sequence specific binding to messenger RNA (mRNA), triggering either translational repression or RNA degradation. It has been predicted that mammalian miRs regulated about 30% of all protein-coding genes (5). miRs have emerged as key regulators of several cellular processes, including cell differentiation, proliferation, tumor invasion, metastasis and angiogenesis (6,7).

miR-10b was detected to be abnormal in the progression of many tumor types including nasopharyngeal carcinoma (8), pancreatic cancer (9), and colorectal cancer (10). In breast cancer cells, miR-10b was considered to be closely correlated with metastatic behavior, and stimulated *in vitro* and *in vivo* tumor invasion (11). Although breast carcinoma cell lines have been explored, tissue examination of miR-10b expression in breast carcinoma has not been reported yet especially in ANN patients by *in situ* hybridization (ISH). Moreover, the role of miR-10b on angiogenesis was limited in previous studies. In Plummer's study, targeting miR-10b led to significant defects in angiogenesis-mediated tumor growth in mice. Suppression of miR-10b led to significant defects in tube number, length and mobilization in human and murine endothelial cells (7). Accordingly, we sought to determine the relationship between miR-10b and microvessel density (MVD) in human breast cancer, whether miR-10b was differentially expressed between patients with different

characteristics, and whether it could serve as a metastatic marker in ANN breast cancer.

Patients and methods

Study population. We conducted a retrospective review of all consecutive ANN breast cancer patients between January 1, 2004 and December 31, 2006 treated in the Tianjin Medical University Cancer Institute and Hospital (Tianjin, China). A total of 1,265 cases were collected with primary, operable, invasive carcinoma, without axillary lymph node and other sites involvement. Among them, a total of 893 cases were diagnosed as invasive ductal carcinoma (IDC) based on paraffin-embedded slices after operation. The pathological stage of tumor was assessed according to the criteria established by the 7th edition of the American Joint Committee on Cancer (AJCC) staging manual. Histological grades of the tumors were designated as I-III according to Elston and Ellis' criterion (12). Peritumoural vascular invasion was assessed following the recommendation by Rosen and Obermann (13).

The follow-up contacts were applied at 3-month intervals over the first year, 6-12 months for the following 4 years, and then annually. The medical work-up consisted of regular physical checkups, imaging tests such as chest X-ray, bone scan and/or ultrasound, to detect recurrence, second primary tumor, or metastatic disease. According to 5-10 years follow-up, we found that 65 ANN cases diagnosed as IDC developed distant metastasis, or even died of the disease, who were defined as 'poor group', with the median follow-up time of 97.8 months for patients alive. Meanwhile, 70 patients were observed with local recurrence, and the other 758 patients were on recurrence-free survival fortunately. A case-control study was designed by stratified sampling method (14,15) depending on the patients age (pre-menopause and post-menopause), and the tumor size of the 'poor group'. Each case in the poor group was matched by 2 cases from the 758 progression-free patients. A total of 130 patients were randomly selected and served as control group ('good group'), with the median follow-up time of 98.3 months. We also gathered data on family history, vascular invasion, tumor grade, treatment application, and recurrence status by chart review.

ISH assay and evaluation of the staining. ISH assay was carried out with probes for miR-10b (5'-CACAAATTCGGT TCTACAGGGTA-3', probe concentration 80 nM) as well as positive control (U6, hsa/mmu/rno) and negative control (scramble-miR) purchasing from Exiqon (Vedbek, Denmark). Four micron paraffin sections fixed to glass slides were baked, dewaxed, hydrated, washed and then incubated in pepsin solution for 15 min at 37˚C, fixed in 4% paraformaldehyde for 10 min and washed in PBS buffer twice for 10 min. Prehybridization solution was dropped onto the slides and reacted (42˚C) in a hygro-cabinet to keep them moist. After 2 h, superfluous prehybridization solution was discarded and digoxigenin-labeled miR-10b probediluted with hybridization solution was denatured for 5 min at 95˚C. Hybridization was performed in a humid chamber for 16 h at 45˚C. After hybridization, the parafilms were removed by stringency washes twice with 2X SSC at 37˚C for 5 min, and then the sections were in 0.5X SSC at 37˚C for 15 min, 0.2X SSC at 37˚C for 15 min. Then, the slides were placed in a blocking solution for 30 min at 37˚C, and incubated for 1 h at room temperature with monoclonal anti-Digoxin Biotin Conjugate (Boster Bio, Co., Ltd., Wuhan, China). After washing in PBS, they were incubated for 20 min with strept-avidin biotin complex (SABC) at 37˚C. After washing again with PBS, biotinylation peroxydase was added for 20 min at 37˚C. Afterwards, the assay was colored by diaminobenzidine, counterstained with hematoxylin, dehydrated in a gradient of alcohols, and mounted.

The positive signal of miR-10b was a brown precipitate at sites of hybridization, which was evaluated by the German semiquantitative scoring system combining intensity of cytoplasmic staining and number of positive cells (16). For each sample, a score was given with regard to the percentage of positive cells as follows: None (0 point), 1 to 24% of the cells (1 point), 25 to 49% of the cells (2 points), 50 to 74% of the cells (3 points), and 75 to 100% of the cells (4 points). Another score was given for the intensity of staining cells as follows: None (0 point), weak staining (1 point), intermediate staining (2 points), and strong staining (3 points). A final score was then calculated by multiplying the above two scores. If the final score was 4 or more, expression was considered to be positive.

Immunohistochemical (IHC) assay and evaluation of the staining. IHC stainings were performed on formalin-fixed, paraffin-embedded samples obtained from the pathology registry. Primary antibody used in this study included estrogen-receptor (ER; SP1, 1:200 dilution; Zeta Corp., Sierra Madre, CA, USA), progesterone-receptor (PR; SP2, 1:200 dilution; Zeta Corp.), human epidermal growth factor receptor 2 (HER2; CB11, 1:100 dilution; Invitrogen; Thermo Fisher Scientific, Inc., Waltham, MA, USA), Ki67 (K-2, 1:100 dilution; Invitrogen; Thermo Fisher Scientific, Inc.), and CD34 (EP88, 1:150 dilution; Abcam, Cambridge, MA, USA). The immunostaining was scored double blindly by two pathologists, who were blinded to patients' clinicopathologic characteristics and outcomes. For each antibody, the location of immunoreactivity, percentage of stained cells, and intensity were determined. ER and PR were categorized as negative (<1%) and positive (≥1%), in accordance with the guidelines (17). For HER2, the IHC score was assigned according to the American Society of Clinical Oncology/College of American Pathologists (ASCO/CAP) guideline (18). HER2-positive cases were defined as IHC score of 3+ or IHC score of 2+ plus fluorescent ISH with amplification ratio ≥2.0. Ki67 status was expressed in terms of percentage of positive cells, with a threshold of 14% of positive cells (19). The criteria for subtype classification were as follows (20): 'luminal A-like' (ER positive and PR ≥20% and HER2 negative and Ki-67 <14%), 'luminal B-like (HER2 negative)' (ER positive and HER2 negative and at least one of: Ki-67 ≥14% or PR <20%), 'luminal B-like (HER2 positive)' (ER and HER2 positive, with any Ki67 and PR), 'HER2 positive' (ER and PR negative and HER2 positive), 'triple negative' (ER and PR negative and HER2 negative).

MVD was determined by the number of microvessels positive for CD34, whose label could be observed in the cytoplasm of endothelial cells. MVD scoring was based on a modification of the method described by Weidner *et al* (21) in which large microvessels and any single brown-staining endothelial cell

clearly separated from adjacent microvessels, tumor cells, and other connective tissue elements were considered a single and countable microvessel. The entire tumor section was scanned at low magnification (x40) to identify the area of highest vessel density (hot spot). The five most prominent vascular areas within the tumor mass were chosen. Microvessels in each hot spot were counted in a single x200 field and the average counts of the 5 fields were recorded and defined. Vessel lumen was not required for identification of a microvessel. Single cell or cell clusters were counted. Branching structures were counted as single vessel. Large vessels with thick muscular walls or with lumina greater than 50 μm were excluded from the count. Discrepant cases were reviewed by the pathologists group, and the consensus results were used for the analysis.

Statistical analysis. The SPSS software (version 17.0 for Windows) was used to carry out the statistical analyses. Normal distribution of the age and MVD total scores was assessed using the Kolmogorov-Smirnov test. Comparison of MVD between different groups was performed by ANOVA test. Correlations between two variables were evaluated by Spearman's rank-correlation test. The correlation analyses between groups were examined by the χ^2 test. The multivariate analysis used a logistic multiple regression model. A two-sided P<0.05 was considered statistically significant in all of the analyses except subdividing RxC table in χ^2 test.

Results

Patient cohort. For 65 cases with 'poor group', all of them developed distant metastases (including bone, lung, liver, brain, bone marrow, or other organs). These recurrent sites were detected and proven through roentgenography, sonography, computed tomography, radioisotope scanning, magnetic resonance imaging, or puncture biopsy. A total of 45 cases among them developed cancer-specific death. Clinicopathologic features were presented in Table I. Among all patients, significant differences were found in peritumoural vascular invasion, grade and molecular subtype between 'poor' and 'good' groups (P<0.05). Invasion of peritumoural vascular vessels and poor differentiation were strictly correlated with recurrence (P=0.017 and P=0.031, respectively). 'Luminal A-like' subtype accounted for about 36.9% in the 'good group', but only 16.9% in the 'poor group'. Among the 'good group', 21.5% were 'luminal B-like (HER2 negative)', 10.0% 'luminal B-like (HER2 positive)', 8.5% 'HER2 positive', and 23.1% 'triple negative'. While among the 'poor group', the percentage of the five subtypes were 16.9, 20.0, 12.3, 18.5, and 32.3%, respectively. Distribution of subtypes between groups was different with statistical significance (P=0.026). As mentioned in the 'Patients and methods', stratified sampling method was applied, so no significant difference was found in age, tumor size, menopausal status (P>0.05). Treatment including chemotherapy, endocrine therapy and radiotherapy didn't show statistical differences between the two groups (P>0.05).

IHC staining of CD34 and ISH of miR-10b in breast cancer tissues were illustrated in Fig. 1. Microvessels were located predominantly in the stroma surrounding the tumor nests. Among all cases, greater percentage of cases displayed cytoplasm staining for miR-10b in 'poor group' (73.8%) than in 'good group' (51.5%, P=0.003), and MVD count was higher in 'poor' cases than in 'good' cases (P<0.001; Table II).

Univariate analysis showed that clinicopathologic indicators such as tumor grade, peritumoural vascular invasion and molecular subtype were correlated with distant metastasis (P<0.05). To further assess the independence of the prognostic value of miR-10b expression, these indicators were analyzed with a multivariate logistic regression model. As shown in Table III, miR-10b retained independent prognostic significance (OR 2.575, 95% CI, 1.323-5.012; P=0.005) along with MVD (OR 3.067, 95% CI, 1.605-5.861; P=0.001) which were adjusted by peritumoural vascular invasion. The significant influence on distant metastasis by histological grade and subtypes was not confirmed in the logistic analysis.

Among all of the 195 patients with ANN disease, high MVD was associated closely with poor histological grade, existence of vascular invasion, as well as 'triple negative' subtype (P<0.05), but did not show any relationship with age and tumor size (Table IV). Meanwhile, we found that the expression of miR-10b was significantly associated with tumor grade, tumor size and subtypes (P<0.05). The subdividing RxC table in χ^2 test was used to evaluate the association between two indicators. miR-10b positive rate was upregulated from grade 1 (53.8%) and grade 2 (53.9%) to grade 3 (78.0%, χ^2=7.517, P=0.006), and its expression between T2 and T1a+1b (χ^2=5.702, P=0.017) remained significant difference. Meanwhile, among patients with 'HER2 positive' subtype, miR-10b expression rate was 78.3% (18 of 23 cases), whereas only 16 of 59 cases (27.1%) with 'luminal A-like' subtype. Expression of miR-10b rose from 'luminal A-like' to 'luminal B-like (HER2 negative)' to 'triple negative' to 'luminal B-like (HER2 positive)' to 'HER2 positive', and the differences between 'luminal A-like' and 'luminal B-like (HER2 negative)' (χ^2=14.81, P<0.001), 'luminal A-like' and 'triple negative' (χ^2=24.58, P<0.001), 'luminal A-like' and 'luminal B-like (HER2 positive)' (χ^2=15.53, P<0.001), 'luminal A-like' and 'HER2 positive' (χ^2=17.84, P<0.001) were significant. However, the expression of miR-10b between other subtypes did not demonstrate statistical difference (P>0.005).

miR-10b expression was positively associated with the MVD count (r=0.370, P<0.001), tumor grade (r=0.168, P=0.019) and tumor size (r=0.175, P=0.014), and negatively associated with age (r=-0.146, P=0.042). No significant associations were identified between the expression of miR-10b and vascular invasion (r=0.076, P=0.292), or intrinsic subtypes (r=0.011, P=0.875; Table IV).

In addition, ROC analysis was performed. As illustrated in Fig. 2, the area under the curve (AUC) is 0.760, 95% CI, 0.686-0.834, P<0.0001. And the sensitivity and specificity of MVD for recurrence of breast cancer is 0.508 and 0.900, respectively.

In the 97.8-month interval, patterns of distant metastasis divided by expression status of miR-10b for cases in the 'poor group' were demonstrated in Fig. 3. Bone was the predominant site of metastasis for the two groups (64.7% in miR-10b-negative tumors and 43.8% in miR-10b-positive tumors, respectively). Meanwhile, occurrence rate of distant metastasis was 29.4% (5/17) in lung, 17.6% (3/17) in liver, 23.5% (4/17) in distant lymph node, 5.9% (1/17) in brain, and

Table I. Characteristic of the ANN patients with poor and good prognosis.

Characteristic	Total	Poor prognosis	%	Good prognosis	%	P-value
All	195	65		130		
Age at diagnosis, years						
<35	5	2	3.1	3	2.3	
35 to <49	94	31	47.7	63	48.5	
>50	96	32	33.3	64	49.2	>0.05
Mean ± SD		54.0±10.2		54.1±10.1		>0.05
Menopausal status						
Premenopausal	92	30	46.2	62	48.0	
Postmenopausal	103	35	53.8	68	52.0	>0.05
Tumor size						
T1a+T1b	6	2	3.1	4	3.1	
T1c	40	14	21.5	26	20.0	
T2	137	45	69.2	92	70.8	
T3	12	4	6.2	8	6.1	>0.05
Family history						
Yes	29	9	13.8	20	15.4	
No	166	56	86.2	110	84.6	>0.05
Peritumoural vascular invasion						
Absent	176	54	83.1	123	94.6	
Present	19	11	16.9	7	5.4	0.009
Tumor grade						
Low	26	5	7.7	21	16.2	
Intermediate	128	40	61.5	88	67.7	
High	41	20	30.8	21	16.2	0.031
Molecular subtype						
'Luminal A-like'	59	11	16.9	48	36.9	
'Luminal B-like (HER2 negative)'	41	13	20.0	28	21.5	
'Luminal B-like (HER2 positive)'	21	8	12.3	13	10.0	
'HER2 positive'	23	12	18.5	11	8.5	
'Triple negative'	51	21	32.3	30	23.1	0.026
Chemotherapy						
Yes	152	52	80.0	100	76.9	
No	43	13	20.0	30	23.1	>0.05
Radiotherapy						
Yes	48	15	23.1	33	25.4	
No	147	50	76.9	97	74.6	>0.05
Endocrine therapy						
No. of ER positive subtype	121	32	49.2	89	68.5	
Yes	108	28	43.1	80	61.5	
No	13	4	6.1	9	7.0	>0.05

Statistical tests for categorical variables were performed using the χ^2 test; mean age was tested using the Mann-Whitney test. ANN, axillary lymph node-negative; HER2, human epidermal growth factor receptor 2; ER, estrogen-receptor.

17.6% (3/17) in other sites for those miR-10b-negative tumors. Among the patients with miR-10b-positive tumors, the rates of metastasis in lung (41.6%), liver (31.2%), distant lymph node (33.3%), brain (15.8%), and other sites (20.8%) were higher to some extent. It seemed that visceral metastasis was more frequently found in the miR-10b positive group.

Discussion

miR-10b is known to function as an oncogene in various kinds of cancers. It has been reported that miR-10b is highly expressed in metastatic cancer cells propagated as cell lines as well as in metastatic breast cancer patients (11). One of the

Table II. MVD (detected by IHC of CD34) and miR-10b expression (detected by ISH) in ANN breast cancer with poor and good prognosis.

		MVD		miR-10b		
Groups	Number	Mean ± SD	P-value[a]	Positive number	Positive rate (%)	P-value
Good prognosis	130	30.81±10.68	<0.001	67	51.5	0.003
Poor prognosis	65	47.82±16.30		48	73.8	

[a]ANOVA test. MVD, microvessel density; IHC, immunohistochemical; ISH, *in situ* hybridization; ANN, axillary lymph node-negative.

Table III. Logistic multiple regression analysis comparing patients with poor and good prognosis.

					95% CI	
Variables	β	SE	Sig (P)	Expβ	Lower	Lower
MVD[a]	1.121	0.330	0.001	3.067	1.605	5.861
miR-10b[a]	0.946	0.340	0.005	2.575	1.323	5.012

[a]Peritumoural vascular invasion-adjusted. MVD, microvessel density.

representative targets of miR-10b was HOXD10, whose inhibition led to activation of the pro-metastatic gene RHOC (22). Recently, in addition to its metastasis-promoting role, the angiogenesis effect of miR-10b has been reported. Shen *et al* demonstrated a role of miR-10b in regulating angiogenesis specifically in response to thrombin through down regulation of HOXD10 (23).

We undertook the study to explore the role of miR-10b in tumor prognosis, its significance in different subtypes, and the relationship between miR-10b and MVD in ANN breast cancer. Our data clearly showed that miR-10b expression was a common feature of invasive breast carcinoma in a Chinese population. Among 195 interpretable cases with IDC, 59.0% were positive for miR-10b expression. Besides, miR-10b was found in 51.5% patients with recurrence-free and 73.8% with metastasis breast cancer cases (P=0.003; Table II). The presented data showed that patients whose tumors did not express miR-10b had more favorable prognosis than those with positive expression. Accordingly, the miR-10b may play a critical role in breast cancer metastasis.

This study further indicated that positive miR-10b expression contributed to poorer differentiation and larger tumor size. miR-10b expression was gradually upregulated from grade 1 (53.8%) and grade 2 (53.9%), to grade 3 (78.0%), and from T1c (51.0%) to T2 (63.5%) and T3 (69.2%). In addition, miR-10b expression was decreased in 'luminal A-like' subtype, which was confirmed to represent excellent prognosis (24). A logistic multiple regression analysis was also carried out and indicated miR-10b could predict prognosis independently. These potentially suggested the promotion effect of miR-10b on breast tumor growth and metastasis. It has been reported that miR-10b expression was correlated with high-grade malignancy in various cancer types (25). Zhao *et al* (26) measured

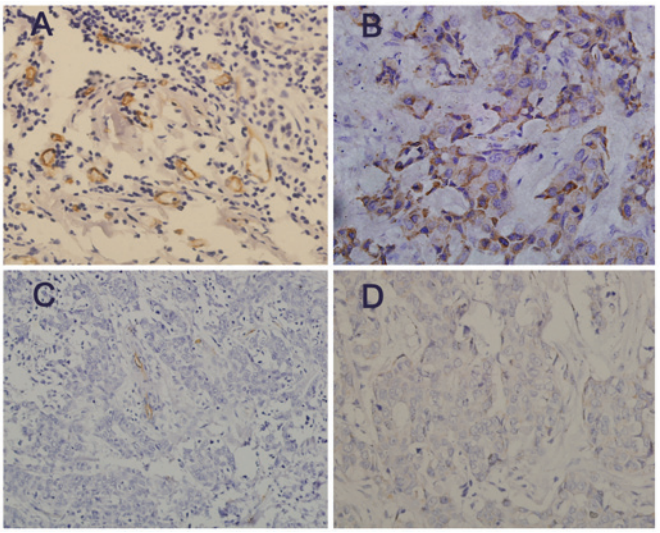

Figure 1. Immunohistochemistry of CD34 and *in situ* hybridization of miR-10b in breast invasive ductal carcinoma tumor of different prognosis. (A) (Magnification, x20) and (B) (magnification, x40) demonstrated the tissues of an ANN patient in the 'poor group' with 8-month metastasis-free survival. The endothelial cells expressed CD34 antigens were widely distributed in the stroma and also tumor cells were positive for miR-10b. (C) (Magnification, x20) and (D) (magnification, x40) demonstrated the tissues of an ANN patient in the 'good group' with progression-free survival of 82 months. Less endothelial cells expressed CD34 were observed and tumor cells were negative for miR-10b. ISH, *in situ* hybridization; ANN, axillary lymph node-negative.

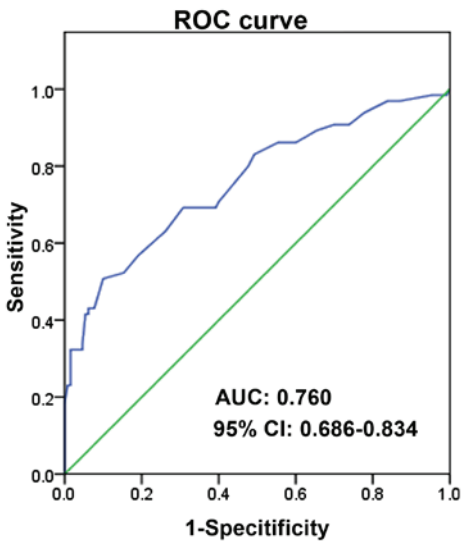

Figure 2. ROC curve for MVD. MVD, microvessel density.

Table IV. MVD (detected by IHC of CD34) and miR-10b expression (detected by ISH) with clinicopathologic features of 195 cases.

		MVD		miR-10b				
Indicator	Number	Mean ± SD	P-value	Positive number	Positive rate	P-value[c]	r	P-value[d]
Age								
<35	5	37.60±8.26		3	60.0			
35 to <49	94	39.2±14.50		63	67.0			
>50	96	37.1±14.61	0.796[a]	49	51.0	0.057	-0.146	**0.042**
Grade								
Grade 1	26	35.4±12.32		14	53.8			
Grade 2	128	37.3±14.58		69	53.9			
Grade 3	41	43.8±14.00	**0.023[a]**	32	78.0	**0.020**	0.168	**0.019**
Tumor size								
T1a+T1b	5	31.20±13.52		0	0			
T1c	51	37.67±12.94		26	51.0			
T2	126	38.44±15.2		80	63.5			
T3	13	44.77±10.22	0.271[a]	9	69.2	**0.015**	0.175	**0.014**
Peritumoural vascular invasion								
Absent	175	36.92±13.37		101	57.7			
Present	20	52.10±16.20	<0.001[a]	14	70.0	0.290	0.076	0.292
Molecular subtype								
'Luminal A-like'	59	32.69±10.86		16	27.1			
'Luminal B-like (HER2 negative)'	41	36.78±13.03		27	65.9			
'Luminal B-like (HER2 positive)'	21	38.29±15.00		16	76.2			
'HER2 positive'	23	38.74±11.78		18	78.3			
'Triple negative'	51	46.49±16.52	**<0.001[b]**	38	74.5	**<0.001**	0.011	0.875
miR-10b expression								
Positive	115	42.40±14.05						
Negative	80	32.84±13.02	**<0.001[a]**			MVD	0.370	**<0.001**

[a]P-values were calculated by ANOVA test. The sequence of the different grade: Grade 1 = grade 2 (P=0.520) < grade 3 (P=0.013) (multiple comparision in ANOVA). [b]Comparison of MVD in 5 molecular subtypes: P-values were calculated by Kruskal-Wallis test (λ^2=21.79); luminal A < triple negative (P<0.001, Mann-Whitney U test). [c]P-values were calculated by χ^2 test. The sequence of the different grade: Grade 1 = grade 2 (P=0.9967) < grade 3 (P=0.006<0.017, subdividing RxC table in χ^2 test); the sequence of the different tumor size: T1a and T1b<T2 (P=0.017<0.008, subdividing RxC table in χ^2 test); the sequence of the different subtypes: Luminal A < luminal B (P<0.001<0.005) = triple negative (P=0.365) = luminal HER2 (P=0.881) = HER2 enriched (P=0.870) (subdividing RxC table in χ^2 test). [d]P-values were calculated by Spearman's rank-correlation test (n=195). Bold values indicate statisical significane where P<0.05. MVD, microvessel density; IHC, immunohistochemical; ISH, *in situ* hybridization; HER2, human epidermal growth factor receptor 2.

serum miR-10b in 122 breast cancer patients with or without bone metastases. The results showed that serum miR-10b concentrations were significantly higher in patients with bone metastases than those without metastasis. This finding was more or less consistent with our research. Furthermore, in a study by Ma *et al* (11), to determine whether miR-10b expression correlated with clinical outcome in patients, they measured its levels in primary tumor samples from 23 breast cancer patients by RT-PCR. When compared with normal breast tissue, miR-10b expression level was lower in all of the breast carcinomas from metastasis-free patients (5/5). In contrast, 50% of the metastasis-positive patients (9/18) had elevated miR-10b levels in their primary tumors (P=0.03), which were also in consonance with our study. In research of breast cancer cells, the mechanism of metastasis seemed to be associated with expression levels of the epithelial-mesenchymal transition (EMT)-inducing and metastasis-promoting transcription factor Twist. In mammary epithelial cells and breast carcinoma cells, miR-10b could directly suppress the translation of HOXD10, an mRNA encoding a transcriptional repressor that inhibited expression of several genes such as RHOC, urokinase plasminogen activator receptor, α3-integrin, and MT1-MMP, which were involved in cell migration and extracellular matrix remodeling (11).

Besides the expression of miR-10b, we also measured MVD count labeled by CD34 of all patients. MVD represented the

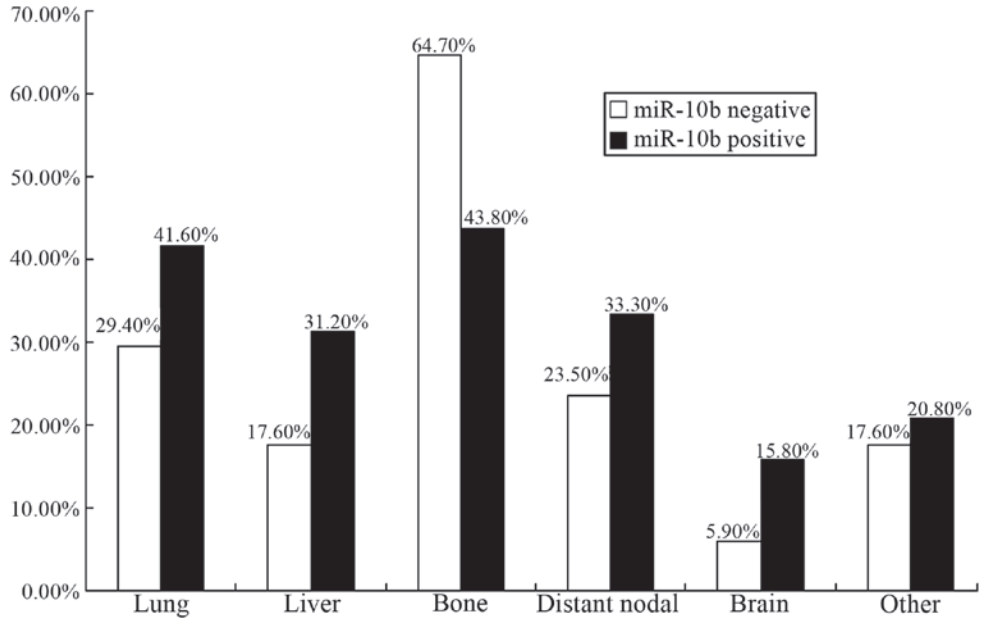

Figure 3. Patterns of distant metastasis according to miR-10b expression among patients with poor prognosis. Distant recurrence may occur in one or more of the sites listed. Individual patients may be counted more than once.

degree of tumor neovascularization, and it had been found to be an important indicator of malignant behavior in breast cancer (27). Among all the patients, the mean value of MVD was 38.48±14.40, which was different with statistical significance between patients in 'good group' (30.81±10.68) and patients in 'poor group' (47.82±16.30, P<0.001). Furthermore, results indicated that the patients with good differentiation, absence of vascular invasion or 'luminal A-like' subtype were correlated with low MVD count, consistent with the recent studies (28,29). The logistic multiple regression analysis also detected MVD as an independent prognostic marker for metastasis.

Moreover, the presented data showed a significantly positive correlation between miR-10b and MVD count (r=0.370, P<0.001), indicating that miR-10b expression may be a potential marker in predicting angiogenesis. In the study by Plummer *et al* (30), genome-wide deep sequencing of small RNAs revealed miR-10b was significantly upregulated in tumor vasculature. Moreover, suppression of miR-10b led to significant defects in tube number and length, as well as mobilization in human and murine endothelial cells, which was in agreement with an observation showing that miR-10b regulated HOXD10 in microvessels (23). In a study by Myers *et al*, HOXD10 was demonstrated to maintain a nonangiogenic state in the endothelium. Sustained expression of HOXD10 impaired endothelial cell migration and blocked angiogenesis induced by basic fibroblast growth factor and vascular endothelial growth factor in the chick chorioallantoic membrane *in vivo*. HOXD10-overexpressing human endothelial cells also failed to form new vessels when implanted into immunocompromised mice (31). These findings strongly argued for miR-10b's role of promoting angiogenesis. In the future we plan to look into the role of angiogenesis of miR-10b in breast cancer cells and animals, and to explore the possibility of miR-10b as a new target of anti-angiogenesis therapeutic intervention for breast cancer.

In this study, histological grade and subtype were associated with metastasis in univariate analysis. The association, however, was no longer statistically significant after adjusting for other variables. It is probably due to a small sample size and some factors covering and concealing the function of others as a result of a complex relationship.

In conclusion, the study suggested that miR-10b expression was associated with breast cancer aggressive behavior, distant metastasis, angiogenesis and poor prognosis. Further exploration of the clinical significance of miR-10b expression in breast cancer requires larger sample size and prospective studies to confirm the findings of this study. The development of new strategies which can suppress miR-10b will probably lead to clinical benefits not only through anti-metastasis but also through anti-angiogenesis.

Acknowledgements

This study was financially supported by National Science Foundation of China (81172532, 81470119). The authors acknowledge the technological assistance of Mrs. Xiumin Ding and Mrs. Ying Wang.

References

1. Early Breast Cancer Trialists' Collaborative Group (EBCTCG): Effects of chemotherapy and hormonal therapy for early breast cancer on recurrence and 15-year survival: An overview of the randomised trials. Lancet 365: 1687-1717, 2005.
2. Metzger-Filho O, Sun Z, Viale G, Price KN, Crivellari D, Snyder RD, Gelber RD, Castiglione-Gertsch M, Coates AS, Goldhirsch A and Cardoso F: Patterns of recurrence and outcome according to breast cancer subtypes in lymph node-negative disease: Results from international breast cancer study group trials VIII and IX. J Clin Oncol 31: 3083-3090, 2013.
3. Fisher CS, Cole DJ, Mitas M, Garrett-Meyer E, Metcalf JS, Gillanders WE, Mikhitarian K, Urist MM, Mann GB, Doherty G, *et al*: Molecular detection of micrometastatic breast cancer in histopathology-negative axillary lymph nodes fails to predict breast cancer recurrence: A final analysis of a prospective multi-institutional cohort study. Ann Surg Oncol 17 (Suppl 3): S312-S320, 2010.

4. Krol J, Loedige I and Filipowicz W: The widespread regulation of microRNA biogenesis, function and decay. Nat Rev Genet 11: 597-610, 2010.
5. Taft RJ, Glazov EA, Cloonan N, Simons C, Stephen S, Faulkner GJ, Lassmann T, Forrest AR, Grimmond SM, Schroder K, *et al*: Tiny RNAs associated with transcription start sites in animals. Nat Genet 41: 572-578, 2009.
6. Goswami RS, Waldron L, Machado J, Cervigne NK, Xu W, Reis PP, Bailey DJ, Jurisica I, Crump MR and Kamel-Reid S: Optimization and analysis of a quantitative real-time PCR-based technique to determine microRNA expression in formalin-fixed paraffin-embedded samples. BMC Biotechnol 10: 47, 2010.
7. Plummer PN, Freeman R, Taft RJ, Vider J, Sax M, Umer BA, Gao D, Johns C, Mattick JS, Wilton SD, et *al*: MicroRNAs regulate tumor angiogenesis modulated by endothelial progenitor cells. Cancer Res 73: 341-352, 2013.
8. Li G, Wu Z, Peng Y, Liu X, Lu J, Wang L, Pan Q, He ML and Li XP: MicroRNA-10b induced by Epstein-Barr virus-encoded latent membrane protein-1 promotes the metastasis of human nasopharyngeal carcinoma cells. Cancer Lett 299: 29-36, 2010.
9. Setoyama T, Zhang X, Natsugoe S and Calin GA: microRNA-10b: A new marker or the marker of pancreatic ductal adenocarcinoma? Clin Cancer Res 17: 5527-5529, 2011.
10. Jiang H, Liu J, Chen Y, Ma C, Li B and Hao T: Up-regulation of mir-10b predicate advanced clinicopathological features and liver metastasis in colorectal cancer. Cancer Med 5: 2932-2941, 2016.
11. Ma L, Teruya-Feldstein J and Weinberg RA: Tumour invasion and metastasis initiated by microRNA-10b in breast cancer. Nature 449: 682-688, 2007.
12. Elston CW and Ellis IO: Pathological prognostic factors in breast cancer. I. The value of histological grade in breast cancer: Experience from a large study with long-term follow-up. Histopathology 19: 403-410, 1991.
13. Rosen PP and Oberman HA: Tumors of the mammary gland. In: Atlas of Tumor Pathology. 3rd series, fascicle 7. Armed Forces Institute of Pathology, Washington, DC, 1993.
14. Niu Y, Fu X, Lv A, Fan Y and Wang Y: Potential markers predicting distant metastasis in axillary node-negative breast carcinoma. Int J Cancer 98: 754-760, 2002.
15. Zhang L, Wang F, Wang L, Wang W, Liu B, Liu J, Chen M, He Q, Liao Y, Yu X, *et al*: Prevalence of chronic kidney disease in China: A cross-sectional survey. Lancet 379: 815-822, 2012.
16. Koo CL, Kok LF, Lee MY, Wu TS, Cheng YW, Hsu JD, Ruan A, Chao KC and Han CP: Scoring mechanisms of p16INK4a immunohistochemistry based on either independent nucleic stain or mixed cytoplasmic with nucleic expression can significantly signal to distinguish between endocervical and endometrial adenocarcinomas in a tissue microarray study. J Transl Med 7: 25, 2009.
17. Hammond ME, Hayes DF, Dowsett M, Allred DC, Hagerty KL, Badve S, Fitzgibbons PL, Francis G, Goldstein NS, Hayes M, *et al*: American society of clinical oncology/college of American pathologists guideline recommendations for immunohistochemical testing of estrogen and progesterone receptors in breast cancer. J Clin Oncol 28: 2784-2795, 2010.
18. Wolff AC, Hammond ME, Schwartz JN, Hagerty KL, Allred DC, Cote RJ, Dowsett M, Fitzgibbons PL, Hanna WM, Langer A, *et al*: American society of clinical oncology/college of American pathologists guideline recommendations for human epidermal growth factor receptor 2 testing in breast cancer. J Clin Oncol 25: 118-145, 2007.
19. Cheang MC, Chia SK, Voduc D, Gao D, Leung S, Snider J, Watson M, Davies S, Bernard PS, Parker JS, *et al*: Ki67 index, HER2 status, and prognosis of patients with luminal B breast cancer. J Natl Cancer Inst 101: 736-750, 2009.
20. Goldhirsch A, Winer EP, Coates AS, Gelber RD, Piccart-Gebhart M, Thürlimann B and Senn HJ; Panel members: Personalizing the treatment of women with early breast cancer: Highlights of the st Gallen International Expert consensus on the primary therapy of early breast cancer. Ann Oncol 24: 2206-2223, 2013.
21. Weidner N, Folkman J, Pozza F, Bevilacqua P, Allred EN, Moore DH, Meli S and Gasparini G: Tumor angiogenesis: A new significant and independent prognostic indicator in early-stage breast carcinoma. J Natl Cancer Inst 84: 1875-1887, 1992.
22. Ma L: Role of miR-10b in breast cancer metastasis. Breast Cancer Res 12: 210, 2010.
23. Shen X, Fang J, Lv X, Pei Z, Wang Y, Jiang S and Ding K: Heparin impairs angiogenesis through inhibition of microRNA-10b. J Biol Chem 286: 26616-26627, 2011.
24. van der Hage JA, Mieog JS, van de Velde CJ, Putter H, Bartelink H and van de Vijver MJ: Impact of established prognostic factors and molecular subtype in very young breast cancer patients: Pooled analysis of four EORTC randomized controlled trials. Breast Cancer Res 13: R68, 2011.
25. Baffa R, Fassan M, Volinia S, O'Hara B, Liu CG, Palazzo JP, Gardiman M, Rugge M, Gomella LG, Croce CM and Rosenberg A: MicroRNA expression profiling of human metastatic cancers identifies cancer gene targets. J Pathol 219: 214-221, 2009.
26. Zhao FL, Hu GD, Wang XF, Zhang XH, Zhang YK and Yu ZS: Serum overexpression of microRNA-10b in patients with bone metastatic primary breast cancer. J Int Med Res 40: 859-866, 2012.
27. Keyhani E, Muhammadnejad A, Behjati F, Sirati F, Khodadadi F, Karimlou M, Moghaddam FA and Pazhoomand R: Angiogenesis markers in breast cancer-potentially useful tools for priority setting of anti-angiogenic agents. Asian Pac J Cancer Prev 14: 7651-7656, 2013.
28. Niemiec J, Adamczyk A, Ambicka A, Mucha-Małecka A, Wysocki W, Mituś J and Ryś J: Lymphangiogenesis assessed using three methods is related to tumour grade, breast cancer subtype and expression of basal marker. Pol J Pathol 63: 165-171, 2012.
29. Muhammadnejad S, Muhammadnejad A, Haddadi M, Oghabian MA, Mohagheghi MA, Tirgari F, Sadeghi-Fazel F and Amanpour S: Correlation of microvessel density with nuclear pleomorphism, mitotic count and vascular invasion in breast and prostate cancers at preclinical and clinical levels. Asian Pac J Cancer Prev 14: 63-68, 2013.
30. Plummer PN, Freeman R, Taft RJ, Vider J, Sax M, Umer BA, Gao D, Johns C, Mattick JS, Wilton SD, *et al*: MicroRNAs regulate tumor angiogenesis modulated by endothelial progenitor cells. Cancer Res 73: 341-352, 2013.
31. Myers C, Charboneau A, Cheung I, Hanks D and Boudreau N: Sustained expression of homeobox D10 inhibits angiogenesis. Am J Pathol 161: 2099-2109, 2002.